Density Functional Study of Surface Forces in Solutions Containing Star-Shaped Polymers

Clifford E. Woodward

School of Physical Environmental and Mathematical Sciences, University College, University of New South Wales, Building 22, Australian Defence Force Academy, Canberra ACT 2600, Australia

Jan Forsman*

Theoretical Chemistry, Chemical Centre, P.O. Box 124, S-221 00 Lund, Sweden

Received October 7, 2003; Revised Manuscript Received April 28, 2004

ABSTRACT: Density functional theory is used to study polymer solutions between surfaces in equilibrium with a bulk solution. We investigate the effect on the surface interaction free energy of having star polymers with different numbers of arms. In addition, we consider the role played by the strength of the adsorption potential and the concentration of the polymer molecules. The interaction free energy is found to scale quite well with the number of arms on the stars, and the separation dependence of the interaction scales approximately with the radius of gyration. When the adsorption potential is weak, the polymer molecules are depleted. A free energy barrier is nevertheless present—a phenomenon often referred to as depletion stabilization. The barrier scales with the number of arms on the star polymers.

1. Introduction

The stability of colloidal suspensions is often controlled by the addition of polymer. Both experimental[1−7] and theoretical[8−21] investigations have studied the effects of polymer on surface forces between particles. In addition, computer simulations of polymers between surfaces have enriched our understanding of these systems. Surface interactions have been been investigated by us recently using density functional theory.[22−24] Here we will use density functional theory to study the effect on surface interactions of having star-shaped polymer molecules in the solution. Other theoretical studies have investigated the behavior of star polymers at surfaces.[25−34] This includes some early simulation work.

In this article we will focus on the case of attractive surfaces. Polymer molecules will adsorb onto attractive surfaces to form layers. These will usually impart a repulsive barrier to surface aggregation due to the overlapping of the adsorbed layers as the surfaces approach. However, polymers are also able to bridge between surfaces, giving an attractive contribution to the interaction between the surfaces. The overall behavior of the surface free energy depends on the sum of these effects. Underlying these factors are even more subtle effects, which depend on both the size and geometry of the polymer molecules involved. For example, surfaces restrict the number of configurations that polymer molecules are able to exhibit. The resulting loss in configurational entropy will make the environment at surfaces less favorable to polymer molecules and counters the action of the surface attraction. The strength of the depletion effect will depend on the degree of polymerization of the polymer molecules and, in the case of star polymers, on the number of arms.

In many theoretical treatments of polymer solutions, the solvent enters the description implicitly. This model is appealingly simple. Nevertheless, in many circumstances this may be a poor description of a system where the major constituent is the solvent. For example, fundamental thermodynamic phenomena, such as transitions between binary phases, which may be induced by the surfaces, cannot be described by an implicit solvent model. In this work, we will use an explicit solvent model within the density functional theory framework.

Several different versions of density functional theory for polymeric systems have been proposed in the literature,[35−40] with subsequent further developments.[41−45] An important aspect of these latter theories is that they contain a nonlocal treatment of excluded-volume effects. This nonlocality, which was originally introduced by Nordholm and co-workers in the generalized van der Waals theory of simple fluids,[46] admits an accurate description of packing effects. The polymer density functional theory of Woodward[37] has the same structure as the generalized van der Waals theories, i.e., an equation of state enters the theory explicitly. Connectivity is properly included in the sense that for ideal chains the theory is exact. Even with a very simple equation of state, the theory is able to predict structural properties and surface forces for athermal polymer melts and solutions, with surprisingly high accuracy.[17,37,47,48] Woodward and Yethiraj[43] improved the functional by adopting the generalized Flory−Dimer (GFD) equation of state,[49−51] which has been shown to be to be very accurate when compared with simulations of short athermal polymers.[50,52] In this study, we will employ a recently developed functional,[22] which was derived from an equation of state by Wichert et al.[53]

1.1. Polymer Solution Model and Density Functional Theory. We shall give a brief outline of the density functional theory here. A more detailed description can be found elsewhere.[22,54]

Our model consists of polymer molecules, each with r monomers, and solvent. Both solvent particles and monomers are hard spheres with the same diameter, σ, though the theory is able to treat differently sized particles as well. That is, the polymer molecules are immersed in a good solvent. In the case of star-shaped polymers, the polymer molecule consists of a central

10.1021/ma035508b CCC: $27.50
Published on Web 08/07/2004

monomer with f arms attached, all of equal length, i.e., $r = mf + 1$, where m is the number of monomers in a single arm. The configuration of a polymer molecule is represented as $\mathbf{R} = (\mathbf{r}_1, ..., \mathbf{r}_r)$, where $\mathbf{r}_i$ is the coordinate of monomer i. The total bonding potential is given by $V_b(\mathbf{R})$. This potential defines the architecture of the polymer chains, i.e., linear or star-shaped. For the case of linear polymer molecules, the bonding potential has the form

$$e^{-\beta V_b(\mathbf{R})} \propto \prod_{i=1}^{r-1} \delta(|\mathbf{r}_{i+1} - \mathbf{r}_i| - \sigma_m) \quad (1)$$

where $\delta(x)$ is the Dirac delta function and β is the inverse thermal energy. The generalization of the above function to create star-shaped architectures is accomplished by simply defining the required connectivities between monomers via the delta functions.

The multipoint polymer density distribution is denoted by by $N(\mathbf{R})$, i.e., $N(\mathbf{R})\, d\mathbf{R}$ is the number of polymer molecules having configurations between $\mathbf{R}$ and $\mathbf{R} + d\mathbf{R}$. For a fluid of ideal chains, the exact expression for the free energy functional, $\mathcal{F}_p^{id}$, is[37]

$$\beta\mathcal{F}_p^{id}[N(\mathbf{R})] = \int N(\mathbf{R})(\ln[N(\mathbf{R})] - 1)\, d\mathbf{R} + \beta\int N(\mathbf{R})(V_b(\mathbf{R}) + V_m^{ext}(\mathbf{R}))\, d\mathbf{R} \quad (2)$$

where $V_m^{ext}(\mathbf{R})$ is an external potential, which acts on the monomers. The total free energy will contain ideal terms from the solvent as well as excess contributions due to hard-sphere interactions between the fluid particles. A general expression for the grand potential, Ω, can be written as[37]

$$\beta\Omega[N(\mathbf{R}),n_s(\mathbf{r})] = \beta\mathcal{F}_p^{id}[N(\mathbf{R})] + \int n_s(\mathbf{r})(\ln[n_s(\mathbf{r})] - 1)\, d\mathbf{r} + \beta\mathcal{F}^{ex}(\bar{n}_m(\mathbf{r}), \bar{n}_s(\mathbf{r})] + \int\beta(V_m^{ext}(\mathbf{r}) - \mu_p)n_m(\mathbf{r})\, d\mathbf{r} + \int\beta(V_s^{ext}(\mathbf{r}) - \mu_s)n_s(\mathbf{r})\, d\mathbf{r} \quad (3)$$

where μ_p and μ_s are the polymer and solvent chemical potentials, respectively. In this expression we have written the interaction with the external potential in terms of the monomer and solvent particle densities, which are denoted by $n_s(\mathbf{r})$ and $n_m(\mathbf{r})$, respectively. $\mathcal{F}^{ex}[\bar{n}_m(\mathbf{r}), \bar{n}_s(\mathbf{r})]$ is the excess free energy. Forsman et al.[22] have derived an expression for this functional by integrating an equation of state developed by Wichert et al.[53] Since monomers and solvent particles have equal size, the coarse-grained densities, $\bar{n}_m(\mathbf{r})$ and $\bar{n}_s(\mathbf{r})$, have a particularly simple form:

$$\bar{n}_\alpha(\mathbf{r}) = \frac{3}{4\pi\sigma^3}\int_{|\mathbf{r}-\mathbf{r}'|<\sigma} n_\alpha(\mathbf{r}')\, d\mathbf{r}' \quad (4)$$

This nonlocal formulation for the excluded-volume contribution is able to describe nonuniform fluid structures with reasonable accuracy.[46] The density functional theory does not include intramolecular correlations, apart from the bare bonding constraints between the monomers.

In this work we shall study polymer solutions confined by parallel, flat surfaces separated by a distance h. The planar symmetry simplifies the expressions for the density functional significantly as we need only consider functions which vary in the z-coordinate (perpendicular to the surfaces). The total external potential due to the surfaces is given by the general relation

$$V^{ext}(z) = w(z) + w(h - z) \quad (5)$$

It acts equally on monomers and solvent particles; i.e., we do not consider cases of preferential adsorption in this study. The contribution from each wall is

$$w(z) = Aw^{ref}(z) \quad (6)$$

where A is a parameter that regulates the strength of the potential. It acts on an exponentially decaying reference potential, given by

$$w^{ref}(z) = A^{ref}e^{-z/\tau}w_{L-J}(z) \quad (7)$$

The function $w_{L-J}(z)$ is the usual Lennard-Jones interaction.

$$\beta w_{L-J}(z) = 2\pi\left[\frac{2}{45}\left(\frac{\sigma}{z}\right)^9 - \frac{1}{3}\left(\frac{\sigma}{z}\right)^3\right] \quad (8)$$

This choice of potential makes our results directly comparable to those in a previous study on similar systems.[23] In this work, the value of the decay length τ is fixed to be $\tau/\sigma = 1$, giving rise to a short-ranged surface interaction. A^{ref} is chosen such that the net adsorption of an ideal fluid at a wall with surface potential w^{ref} is identical to the net ideal adsorption with a surface potential w_{L-J}. Specifically, with $\tau/\sigma = 1$, this constraint leads to $A^{ref} \approx 2.7057$.

1.2. Numerical Solution. The equilibrium monomer and solvent density profiles are obtained by minimizing the free energy functional. For example, one obtains the following expression for the equilibrium monomer density profile for a linear polymer:

$$n_m(z) = e^{\beta\mu_p}\sum_{k=1}^{r}\int_0^h \delta(z - z_k)\prod_{i=1}^{r-1}\Theta(|\Delta z_i| - \sigma)\prod_{j=1}^{r} e^{-\lambda(z_j)}\, dz_1...dz_r \quad (9)$$

where

$$\lambda_i(z) = \frac{\partial\beta\mathcal{F}^{ex}}{\partial n_m(z_i)} + \beta\, V^{ext}(z) \quad (10)$$

and $\Theta(x)$ is a step function

$$\Theta(x) = \begin{cases} 1 & x \le 0 \\ 0 & x > 0 \end{cases} \quad (11)$$

The solution to eq 9 can be obtained by using a Picard iteration scheme.[37] This can be efficiently achieved via repeated matrix−vector multiplications, the vector dimension set by the number of grid points used to partition the z-coordinate.[55,56] We used a relatively fine grid spacing of $\delta z = 0.01\sigma$, which gave more than sufficient precision.

We denote the minimized free energy as Ω_{eq}. From this quantity, we can obtain the net solvation free energy per unit area, g_s:

$$g_s = \Omega_{eq}/S + P_b h \quad (12)$$

where P_b is the bulk pressure and S is the surface area.

g_s will approach twice the interfacial tension of the fluid at a single wall. The interaction free energy between the surfaces was obtained by subtracting these surface tension terms, i.e.

$$\Delta g_s = g_s - g_s(h=\infty) \tag{13}$$

In our calculations, $g_s(h=\infty)$ was reliably estimated at $h/\sigma \approx 50$.

The net solvation pressure, P_s, can be obtained as the following derivative

$$P_s = -\frac{\partial g_s}{\partial h} \tag{14}$$

or via the virial expression

$$P_s = -\int_0^h \sum_\alpha n_\alpha(z) \frac{\partial w(h-z)}{\partial h} \, dz - P_b \tag{15}$$

where α = m, s represent monomers and solvent particles, respectively. When attempting to determine the physical mechanisms, which account for the interactions between the surfaces, it is useful to decompose the solvation pressure into the various contributions that act across the plane midway between the surfaces ($z = h/2$).[57] These are the following:

• An entropic contribution, P_{en}, simply given by the total particle density at the midplane

$$\beta P_{en} = n_m(h/2) + n_s(h/2) \tag{16}$$

This term is repulsive and is due to the confinement of the fluid particles in the region between the surfaces.

• A repulsive contribution, P_{coll}, which is due to collisions between particles on either side of the midplane. This term is due to the nonlocal interactions between hard spheres and can be obtained from the excess part of the free energy. We begin by writing the excess free energy in the following very general form

$$\beta \mathcal{F}^{ex} = \sum_\alpha \int_0^h n_\alpha(z) \, a_\alpha^{ex}(z) \, dz \tag{17}$$

Using this expression, we obtain

$$\beta P_{coll} = -\sum_\alpha \sum_\beta \int_{\max(0,h/2-\sigma)}^{h/2} \int_{h/2}^{\min(z+\sigma,h)} n_\alpha(z) \, n_\beta(z') \frac{\partial K(z'-z)}{\partial z'} \left\{ \frac{\partial a_\alpha^{ex}(z)}{\partial \bar{n}_\beta(z)} + \frac{\partial a_\beta^{ex}(z')}{\partial \bar{n}_\alpha(z')} \right\} dz \, dz' \tag{18}$$

where

$$K(z'-z) = \frac{3}{4\sigma^3}(\sigma^2 - (z-z')^2) \tag{19}$$

is the coarse-graining kernel.

• An attractive contribution, P_{acr}, due to particles on one-half of the midplane interacting with the wall on the other side

$$P_{acr} = -\sum_\alpha \int_0^{h/2} n_\alpha(z) \frac{\partial w_\alpha(h-z)}{\partial z} \, dz \tag{20}$$

• An attractive contribution, P_{bridge}, due to monomer−monomer bonds bridging across the midplane. For linear polymers, this has the form

$$\beta P_{br} = -2\sum_{i=1}^{r-1} \int_0^{h/2} dz_i \int_{h/2}^{h} dz_{i+1} \int_0^h \prod_{k \neq i,i+1} dz_k \, N(z_1, z_2, ..., z_r) \, \delta(z_{i+1} - z_i - \sigma_m) \tag{21}$$

where $N(z_1, z_2, ..., z_r)$, is the reduced r-point polymer distribution, obtained by integrating over the $x-y$ plane. For star polymers, the expression above is generalized to include all distinct bonded pairs. Bridging attractions arise from polymer molecules that stretch between both surfaces, literally drawing them together. The attraction can be thought of as being due to the loss of configurational entropy that occurs as polymer molecules, adsorbed to both surfaces, are uncoiled when the surfaces are moved apart.

These contributions add to give the total solvation pressure, i.e.

$$P_s = P_{en} + P_{coll} + P_{acr} + P_{bridge} - P_b \tag{22}$$

where P_b is the bulk pressure.

2. Results

In these calculations, the bulk pressure was fixed at $\beta P_b \sigma^3 = 1.690\,382$. This resulted in a bulk solution with a liquidlike density; i.e., the total volume fraction was about 0.26−0.28. It is well-known that oscillatory behavior will be observed in the interaction free energy between surfaces which contain a dense fluid. In the calculations presented below, the polymer concentration is so low that oscillatory forces would be due mainly to the structuring of solvent molecules at the surfaces. However, in the presence of long polymer molecules, nontrivial behavior in the surface free energy occurs at separations much greater than those where structuring would manifest itself in the free energy. At these separations, the interaction free energy is determined mainly by the behavior of the polymer molecules. Nevertheless, as we have seen in earlier work,[22,23] the presence of a solvent can still have a noticeable effect on surface interactions, even at large separations. This is due to the influence that solvent molecules have on the interaction between polymer molecules and surfaces. Despite the fact that solvent and monomer particles have similar interactions with the surfaces, polymer molecules are preferentially adsorbed at larger surface potentials due to the cooperative adsorption of bonded monomers. Another way of viewing this is that the bonded monomers in a polymer molecule suffer a smaller loss in entropy when they adsorb onto surfaces compared with solvent particles. This is because the latter have full translational freedom. However, polymer adsorption is modified by solvent structure at the surfaces, induced by nonlocal hard core effects, as well as the loss of configurational entropy suffered by polymer molecules close to the surfaces.

2.1. Effects of Degree of Polymerization and Number of Arms. In this section we compare the surface interaction free energy, Δg_s, for polymer solutions containing linear and star polymer molecules. The number of arms on the stars and degree of polymerization were varied, using combinations of r = 145, 289, 577 and f = 2, 4, 6, 8. In all cases, the bulk monomer concentration was fixed at $\rho_m^b \sigma^3 = 0.01$. We chose a

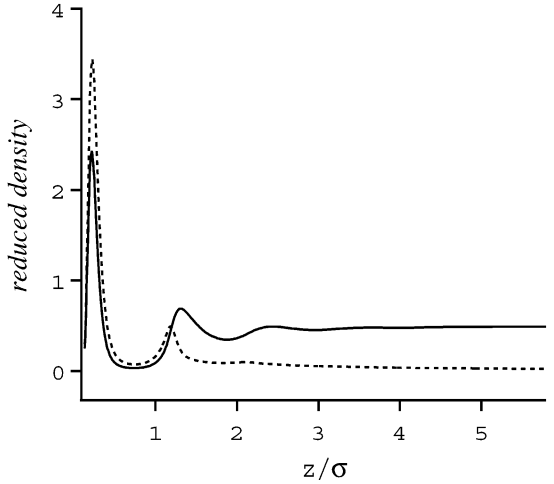

Figure 1. Monomer and solvent reduced density profiles as a function of distance from one surface, when the separation is $h/\sigma = 50$. Densities are in units of σ^{-3}. The dotted curve is the monomer density profile. We show the case of a linear polymer, $f = 2$, with $r = 577$. The bulk monomer density is fixed at $\rho_m^b\sigma^3 = 0.01$, and the surface interaction is $A = 2.0$.

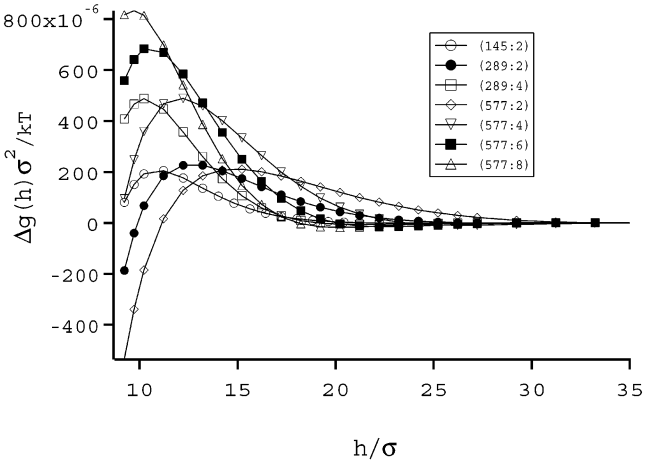

Figure 2. Interaction free energy as a function of separation. The legend indicates the type of polymer molecule in solution with the nomenclature (r: f), where r is the degree of polymerization and f is the number of arms. The bulk monomer density is fixed at $\rho_m^b\sigma^3 = 0.01$, and the surface interaction is $A = 2.0$ for all cases.

surface potential strength of $A = 2.0$ (see eq 6), which gives rise to a significant amount of surface adsorption by polymer molecules. This is illustrated in Figure 1, which shows the monomer and solvent density profiles for the case $r = 577$ and $f = 2$. Significant structuring adjacent to the surface is evident, reflecting the strong adsorption potential as well as hard-sphere packing effects. Very similar density profiles are obtained for star polymers with different numbers of arms.

The results for the interaction free energy are given in Figure 2. There is a similar qualitative shape for the free energy curves for all the parameters. That is, the surface interaction is attractive at short separations, repulsive at intermediate separations, and very weakly attractive at long range. The most noticeable feature is the presence of a free energy barrier at a separation, and with a height, determined by the degree of polymerization and number of arms of the polymer molecules. To understand the mechanisms that underlie the behavior of the free energy, it is useful to consider the various contributions to its derivative, the solvation pressure, as described above.

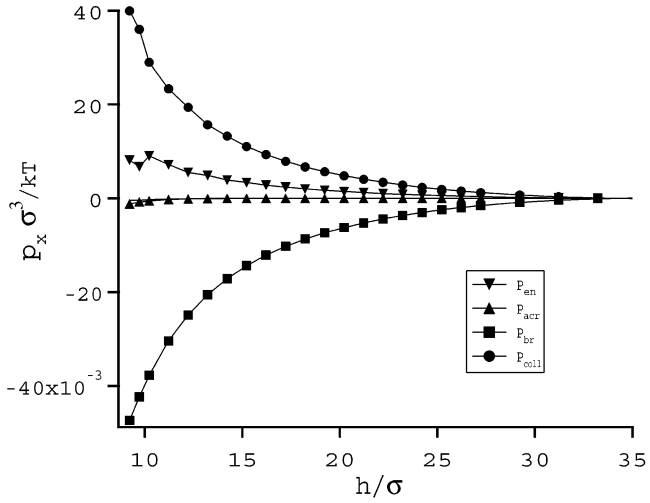

Figure 3. Components of the solvation pressure P_s, as described in the text, for the solution of linear polymers, $r = 577$, described in Figure 1. In all cases, the bulk value for each component has been extracted to give the net component value.

Typical behavior for these contributions is illustrated in Figure 3, which shows the net pressure components for a solution of linear polymers with $r = 577$. At short surface separations, polymer bridging dominates the free energy, with P_{ac} also becoming more important as the separation decreases. At intermediate separations, the repulsive collision and entropic terms become relatively more significant and a free energy barrier builds. However, as the separation increases further, the net pressure components change sign, giving rise to a weakly attractive interaction well beyond the barrier. This change in sign of the pressure components is due to a decrease in the density of polymer molecules at the midplane. This occurs at a separation large enough to hinder bridging by adsorbed polymer molecules but small enough so that molecules from the bulk are not easily able to fill in the resulting density hole around the center of the pore.

The main variation for the interaction free energy for the systems shown in Figure 2 is the separation at which the free energy barrier occurs and the height of the barrier. The position of the barrier depends on the extent that surface adsorbed polymer molecules are able to protrude out into the solution. Increasing the degree of polymerization, r, of the polymers will increase the average coil size. Thus, the barrier occurs at larger separation for longer polymers. However, increasing the number of arms, f, of star polymers (for a fixed degree of polymerization) decreases the size of the polymer coil, and the free energy barrier will occur at smaller separations.

The barrier height is also affected by r and f, though it appears that it is the number of arms, f, which has the largest influence. The entropic, collision, and bridging contributions to the pressure depend on the density of monomers around the midplane. We expect that density would depend approximately linearly with the number of arms. We attempted to quantify the dependence of the interaction free energy on f and r by attempting an approximate, empirical scaling the free energy using these variables. We anticipated that the free energy would scale roughly linearly with the number of arms and that its separation dependence should scale with the size of the loops that an adsorbed polymer molecule projects into the solution. An ap-

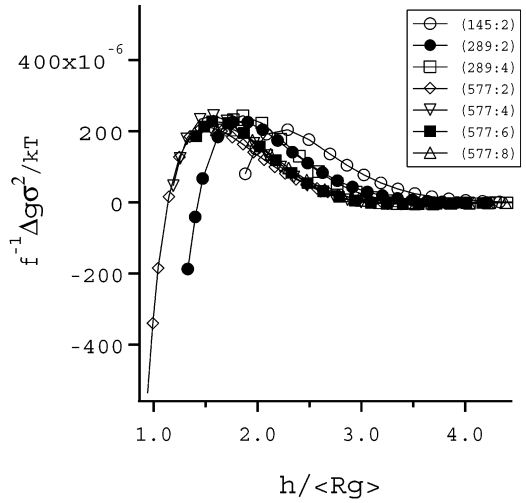

Figure 4. Scaled interaction free energies for the systems described in Figure 1. The free energy is scaled by the number of arms of the polymer molecule, f, and the separation is scaled by the root-mean-square radius of gyration, $\langle R_g \rangle$.

Table 1. Radius of Gyration, R_g, for Various Choices of Polymer Length, r, and Number of Arms, f, As Calculated by Eq 23

r	f	R_g/σ	r	f	R_g/σ
145	2	4.92	577	4	7.75
289	2	6.94	577	6	6.54
289	4	5.49	577	8	5.75
577	2	9.81			

proximate measure for the latter is provided by the mean-square radius of gyration for a star polymer in a θ solvent, which is exactly given by

$$\langle R_g^2 \rangle = \left(\frac{3f-2}{f^2}\right)\frac{r}{6} \tag{23}$$

Relevant examples of R_g for specific choices of r and f are given in Table 1. Using this expression, we applied the following scaling to the data in Figure 2, $\Delta g_s \rightarrow \Delta g_s/f$ and $h \rightarrow h/\sqrt{\langle R_g^2 \rangle}$. The results are given in Figure 4. The magnitude of the free energy does seem to scale reasonably well with the number of arms. Note that we have treated the linear polymer as $f = 2$, rather than $f = 1$, as this preserves the rough scaling of the monomer density discussed above. On the other hand, though scaling distances with the radius of gyration has caused the free energy curves to have similar shapes, they appear to be grouped according to the degree of polymerization of the polymer. The polymers with the higher degree of polymerization display the free energy barrier at shorter scaled separations. The variation in the position of the free energy barrier is most likely related to the extent to which polymer molecules are flattened by the attractive potential of the surfaces. This flattening appears to be greater for polymers with a larger degree of polymerization. Clearly, this effect will not be present in our simple approximation for R_g.

We should note that the scaling relations, proposed here for the free energy, are only empirical in nature, and we make no attempt to rigorously justify our result. Furthermore, we have used only an approximate measure for the polymer radius of gyration, which ignores both surface effects and monomer−monomer repulsions.

2.2. Effect of Surface Potential. In Figure 5, we show the effect on the interaction free energy of varying

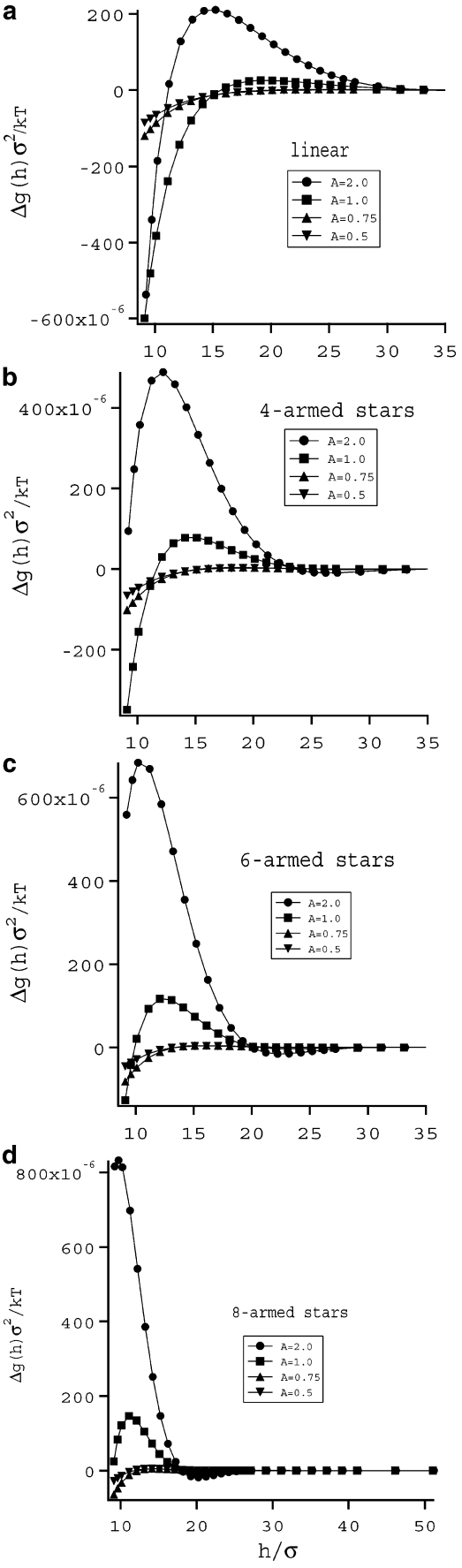

Figure 5. Interaction free energies for various values of the surface potential strength parameter, A. The polymers are linear with $r = 577$. The bulk monomer density is fixed at $\rho_m^b\sigma^3 = 0.01$. (a) Linear polymers, (b) 4-armed stars, (c) 6-armed stars, and (d) 8-armed stars.

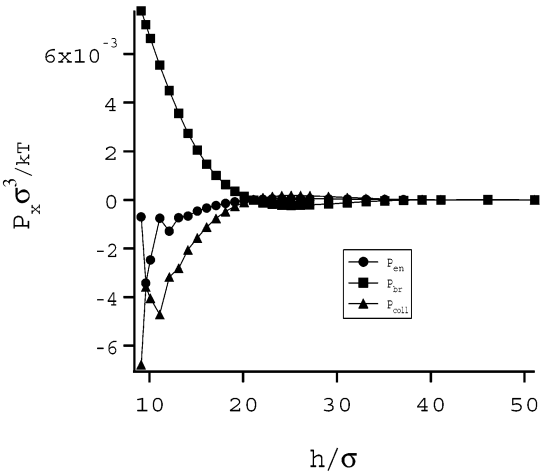

Figure 6. Components of the net solvation pressure as a function of separation for 8-armed stars with $r = 577$. As in Figure 2, the bulk values have been subtracted from each component. The surface potential strength is given by $A = 0.5$, and the bulk monomer density is $\rho_m^b\sigma^3 = 0.01$.

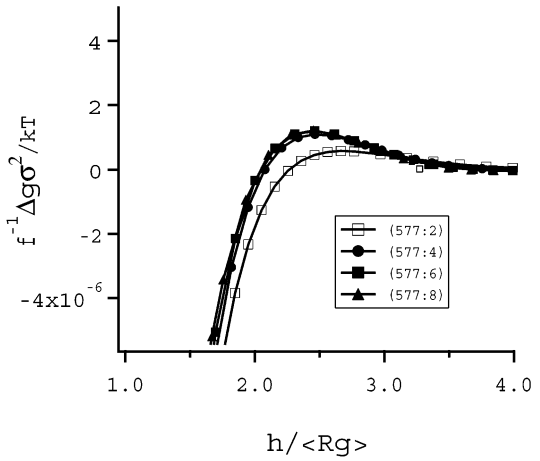

Figure 7. Scaled interaction free energies as described in Figure 3. The legend uses the nomenclature (*r*: *f*), where *r* is the degree of polymerization and *f* is the number of arms. The surface potential strength is given by $A = 0.5$, and the bulk monomer density is $\rho_m^b\sigma^3 = 0.01$.

the potential strength, *A*, acting on the longest polymer ($r = 577$). As the surface strength increases, the free energy barrier increases in height and occurs at a smaller separation. This is due to the higher concentration of adsorbed polymers, giving larger steric and entropic repulsions. In addition, the bridging interactions become stronger. However, more attractive surfaces also cause the polymer molecules to adopt flatter configurations on the surfaces. This has the effect of decreasing the separation at which the bridging attraction becomes important.

It is interesting to note that, at the weakest surface potential, $A = 0.5$, the interaction free energy is predominantly attractive, with only very weak repulsive barriers present. The interaction mechanisms in this system are completely different to those where the surface potential is larger. At $A = 0.5$, the surface attraction is not strong enough to maintain a positive adsorption of polymer molecules, and they become depleted as the surfaces approach one another. This effect is clearly illustrated in Figure 6, which gives the various pressure components as a function of surface separation for 8-armed stars, with $r = 577$. We chose this system, as it displays the largest free energy barrier. Here we see that the components P_{en} and P_{coll} decrease with surface separation, indicating that polymer molecules are depleted from the region between the surfaces. Interestingly, there is some oscillatory structure in these contributions due to hard-sphere packing effects. However, the sum of the entropic and collision contributions is a smooth function, which is monotonically increasing with separation. The depletion effect on these components of the pressure is responsible for the attraction at short separations. On the other hand, the bridging component increases with decreasing separation. That is, bridging gives a net repulsive contribution to the surface interactions, which is completely opposite to the behavior we see between more attractive surfaces. Furthermore, the bridging contribution is sufficiently large at intermediate separations to manifest a free energy barrier. The bridging contribution is more repulsive than would be the case if molecules were simply being removed from the pore created by the surfaces. This suggests that the molecules that remain in the pore contract because of the restrictive environment, leading to a more repulsive bridging contribution. This provides a mechanism for depletion stabilization. In general, our results indicate that the greater the number of arms on the star polymers, the greater is the depletion stabilization barrier. This is supported by a plot of the scaled free energies, Figure 7, which shows that the star polymers appear to satisfy the empirical scaling relationship described in the previous section. However, the linear polymers seem not to follow the universal function.

Measurements of depletion stabilization in polymer solutions, which display some degree of polymer aggregation, have suggested that the repulsive barrier increases with the amount of aggregation.[5,6] This is consistent with our results if we were to assume that aggregated polymers behave similarly to star polymers.

2.3. Bulk Density. The bulk solution determines the chemical potential of the interstitial fluid. The results in this section were obtained by varying the polymer concentration in the bulk, while the solvent density was adjusted so as to keep the pressure of the bulk solution constant at $\beta P_b\sigma^3 = 1.690\,382$. Increasing the density of polymer molecules, while maintaining the bulk pressure, means that the overall density of the solution will usually have to increase. This is because polymer molecules exclude less volume in the fluid than a collection of solvent particles with the same molecular volume.[37]

We consider star polymers with $r = 577$ and $f = 2$, 4, 6, 8. The surface interaction is fixed at $A = 1.0$. The effect of changing the bulk polymer concentration on the interaction free energies for is shown in Figure 8. As the density is increased, the free energy barrier occurs at a smaller separation. The height of the barrier is a nonmonotonic function of the polymer concentration and is largest at $\rho_m^b\sigma^3 = 0.01$. This result can be understood as follows. At low polymer density, not many polymer molecules are adsorbed, and the repulsive steric and entropic contributions are small. Instead, the bridging term will dominate the free energy, giving rise to a small barrier at large surface separation. At larger polymer density, the greater number of polymer molecules, as well as an increase in packing effects (due to the higher overall fluid density), leads to stronger polymer adsorption. However, the adsorbed polymer chains lie flatter

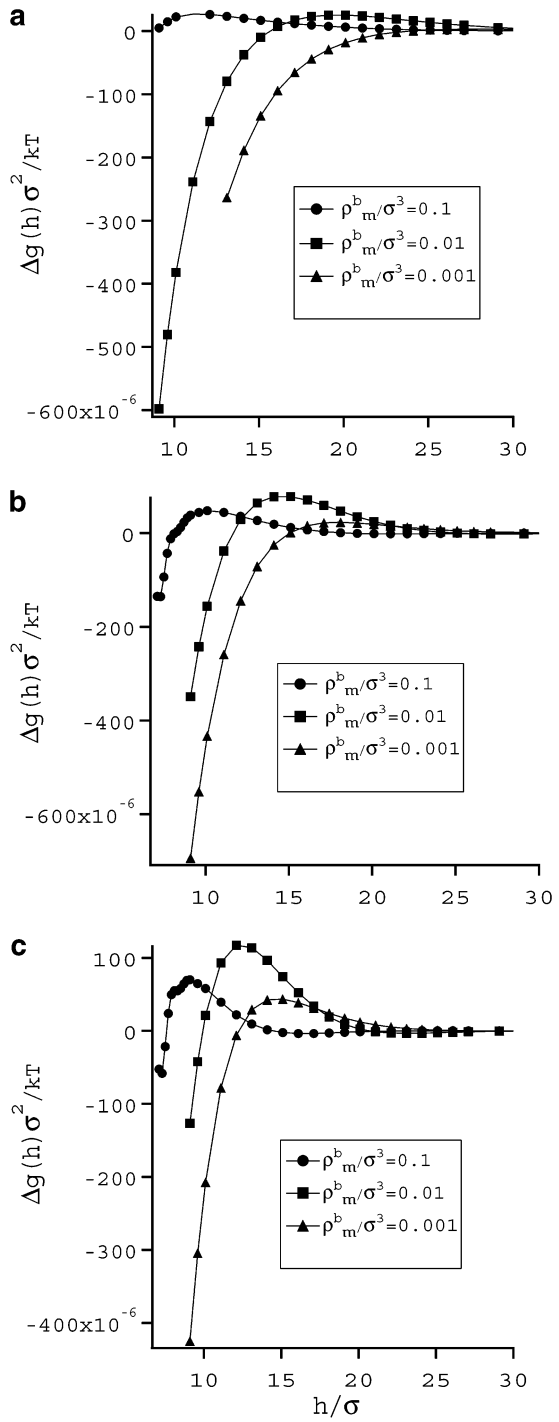

Figure 8. Interaction free energies for various values of the bulk monomer density. The potential strength is given by $A = 1.0$ and $r = 577$. (a) Linear polymers, (b) 4-armed stars, and (c) 6-armed stars.

on the surfaces. This means that the net collision and entropic contributions to the free energy are larger but will be of shorter range. This is illustrated in Figure 9, which gives the pressure components at the highest and lowest polymer concentrations for 4-armed stars. The bridging interactions are also seen to be of shorter range at the higher concentration. The net result is a free energy barrier that moves to smaller surface separations, while the sum of the repulsive and attractive forces may actually decrease the barrier height. The scaled free energies are given in Figure 10. Though it is not perfect, the scaling relationship is a useful guide to the behavior of the interaction free energy.

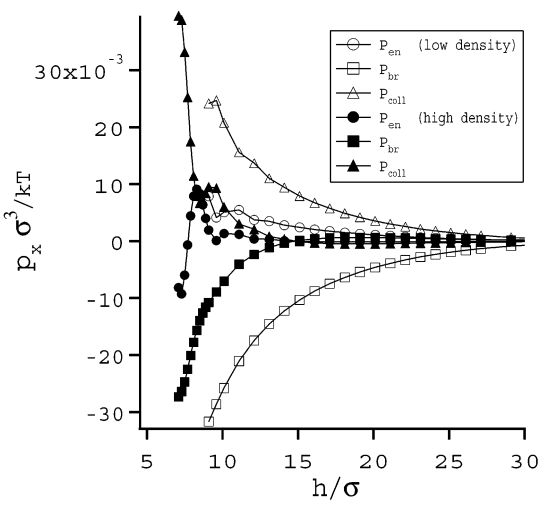

Figure 9. Net components of the solvation pressure for the highest and lowest bulk monomer densities, $\rho^b_m\sigma^3 = 0.1$ and 0.001, for four-armed stars with $r = 577$. In both cases, the surface potential strength is $A = 1.0$, and the bulk pressure is $\beta P_b\sigma^3 = 1.690\,382$.

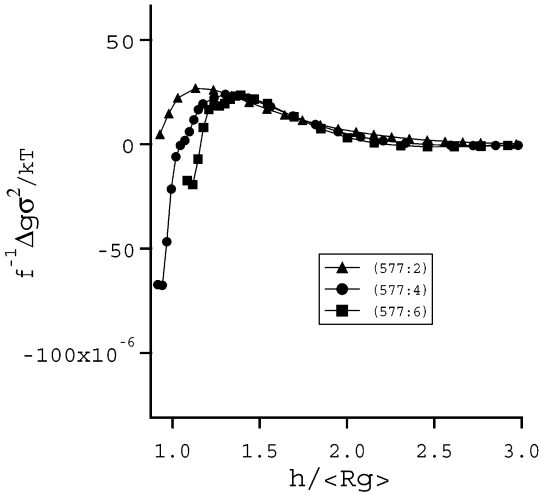

Figure 10. Scaled interaction free energies as described in Figure 3. The legend uses the nomenclature (*r*: *f*), where *r* is the degree of polymerization and *f* is the number of arms. The surface potential strength is given by $A = 1.0$, and the bulk monomer density is $\rho^b_m\sigma^3 = 0.1$.

3. Conclusion

In this article we have used density functional theory to investigate the interaction between surfaces immersed in dilute polymer solutions. In particular, we have compared linear and star-shaped polymers in solution and their influence on the free energy of interaction between the surfaces. Polymer molecules will display positive adsorption at surfaces that are sufficiently attractive. As the surfaces are brought together, the interaction between the adsorbed layers will give rise to a repulsive barrier in the interaction free energy. At even closer separation, bridging interactions will dominate, giving rise to attractions between the surfaces. Interestingly, for star polymers, the magnitude of the free energy barrier appears to scale with the number of arms. Furthermore, scaling the separation dependence of the interaction free energy with the radius of gyration of the polymer molecule (under Θ conditions) gives rise to interaction curves with similar shapes, though the position of the barrier depends on the degree of polymerization. Polymers with a larger

number of monomers have the barrier occurring at closer separations relative to the radius of gyration. This suggests that these molecules are adsorbed to surfaces with relatively "flatter" configurations.

As the strength of the surface attraction decreases, the polymer molecules are less strongly adsorbed, and the barrier height decreases. This effect is larger the greater the number of arms on the star polymers. At the lowest surface attraction that we considered, polymer molecules were actually depleted from the pore, as the surface separation decreased. Nevertheless, a weak free energy barrier remained. We conclude that this barrier is due to the compression of polymer molecules that remain in the pore. This mechanism provides an explanation for the depletion stabilization phenomenon, and it will be investigated further in future work.

Finally, we considered the effect of increasing the concentration of polymer molecules, while maintaining the bulk pressure. For moderately attractive surfaces, we have found that a higher polymer concentration cause the surface interaction to become shorter-ranged, with a barrier height that is a nonmonotonic function of the concentration. This is due to the fact that polymer molecules adsorb with flatter configurations at higher concentration. Thus, the free energy barrier moves to smaller separation, where it is decreases in magnitude by the more strongly attractive bridging forces.

References and Notes

(1) Patel, S. S.; Tirrell, M. *Annu. Rev. Phys. Chem.* **1989**, *40*, 597.
(2) Hu, H.-W.; Granick, S. *Macromolecules* **1990**, *23*, 613.
(3) Ruths, M.; Yoshizawa, H.; Fetters, L. J.; Israelachvili, J. N. *Macromolecules* **1996**, *29*, 7193.
(4) Kuhl, T.; Guo, Y.; Alderfer, J. L.; Berman, A. D.; Leckband, D.; Israelachvili, J. N.; Wen Hui, S. *Langmuir* **1996**, *12*, 3003.
(5) Kuhl, T. L.; Berman, A. D.; Hui, S. W.; Israelachvili, J. N. *Macromolecules* **1998**, *31*, 8250.
(6) Kuhl, T. L.; Berman, A. D.; Hui, S. W.; Israelachvili, J. N. *Macromolecules* **1998**, *31*, 8258.
(7) Seitz, M.; Park, C. K.; Wong, J. Y.; Israelachvili, J. N. *Langmuir* **2001**, *17*, 4616.
(8) Asakura, S.; Oosawa, F. *J. Chem. Phys.* **1954**, *22*, 1255.
(9) Asakura, S.; Oosawa, F. *J. Polym. Sci.* **1982**, *33*, 183.
(10) Vrij, A. *Pure Appl. Chem.* **1976**, *48*, 471.
(11) Joanny, J.-F.; Leibler, L.; deGennes, P. G. *J. Polym. Sci., Polym. Phys. Ed.* **1979**, *17*, 1073.
(12) deGennes, P. G. *Macromolecules* **1982**, *14*, 637.
(13) deGennes, P. G. *Macromolecules* **1982**, *15*, 492.
(14) Feigin, R. I.; Napper, D. H. *J. Colloid Interface Sci.* **1980**, *74*, 567.
(15) Feigin, R. I.; Napper, D. H. *J. Colloid Interface Sci.* **1980**, *75*, 525.
(16) Scheutjens, J. M. H. M.; Fleer, G. J. *Macromolecules* **1985**, *18*, 1882.
(17) Woodward, C. E. *J. Chem. Phys.* **1992**, *97*, 695.
(18) Semenov, A. N.; Joanny, J.-F. *Europhys. Lett.* **1995**, *29*, 279.
(19) Bonet-Avalos, J.; Joanny, J.-F.; Johner, A.; Semenov, A. N. *Europhys. Lett.* **1996**, *35*, 97.
(20) Broukhno, A.; Åkesson, T.; Jönsson, B.; Vorontsov-Velyaminov, P. *J. Phys. Chem. Phys.* **2000**, *113*, 1.
(21) Czezowski, A. Thesis, ADFA, Canberra, 2001.
(22) Forsman, J.; Woodward, C. E.; Freasier, B. C. *J. Chem. Phys.* **2002**, *117*, 1915.
(23) Forsman, J.; Woodward, C. E.; Freasier, B. C. *J. Chem. Phys.* **2003**, *118*, 7672.
(24) Forsman, J.; Woodward, C. E. *J. Chem. Phys.* **2003**, *119*, 1889.
(25) Yethiraj, A.; Hall, C. K. *J. Chem. Phys.* **2003**, *94*, 3943.
(26) Balazs, A. C. *Acc. Chem. Res.* **1993**, *26*, 63.
(27) Cherepanova, T. A.; Stekolnikov, A. V. *Mol. Phys.* **1994**, *83*, 1065.
(28) Irvine, D. J.; Mayes, A. M.; Griffith-Cima, L. *Macromolecules* **1996**, *29*, 6037.
(29) Guttman, C. M.; Di Marzio, E. A.; Douglas, J. F. *Macromolecules* **1996**, *29*, 5723.
(30) Wesley, R. D.; Cosgrove, T.; Thompson, L. *Langmuir* **1999**, *15*, 8376.
(31) Schnitter, M.; Engelking, J.; Heise, A.; Miller, R. D.; Menzel, H. *Macromol. Chem. Phys.* **2000**, *201*, 1504.
(32) Sikorski, A. *Macromol. Theory Simul.* **2001**, *10*, 38.
(33) Jusufi, A.; Dzubiella, J.; Likos, C. N.; von Ferber, C.; Löwen, H. *J. Phys.: Condens. Matter* **2001**, *13*, 6177.
(34) von Ferber, C.; Holovatch, Y.; Jusufi, A.; Likos, C. N.; Löwen, H.; Watzlawek, M. *J. Mol. Liq.* **2002**, *93*, 151.
(35) Chandler, D.; McCoy, J. D.; Singer, S. J. *J. Chem. Phys.* **1986**, *85*, 5971.
(36) McMullen, W. E.; Freed, K. F. *J. Chem. Phys.* **1990**, *92*, 1413.
(37) Woodward, C. E. *J. Chem. Phys.* **1991**, *94*, 3183.
(38) Selinger, J. V.; Bruinsma, R. F. *Phys. Rev. A* **1991**, *43*, 2910.
(39) Kierlik, E.; Rosinberg, M. L. *J. Chem. Phys.* **1992**, *97*, 9222.
(40) Kierlik, E.; Rosinberg, M. L. *J. Chem. Phys.* **1993**, *99*, 3950.
(41) McCoy, J. D.; Honnell, K. G.; Schweizer, K. S.; Curro, J. G. *J. Chem. Phys.* **1991**, *114*, 9348.
(42) Kierlik, E.; Rosinberg, M. L. *J. Chem. Phys.* **1992**, *100*, 1716.
(43) Woodward, C. E.; Yethiraj, A. *J. Chem. Phys.* **1994**, *100*, 3181.
(44) Yethiraj, A.; Woodward, C. E. *J. Chem. Phys.* **1995**, *102*, 5499.
(45) Yethiraj, A. *J. Chem. Phys.* **1998**, *109*, 3269.
(46) Nordholm, S.; Johnson, M.; Freasier, B. C. *Aust. J. Chem.* **1980**, *33*, 2139.
(47) McCoy, J. D.; Teixeira, M. A.; Curro, J. G. *J. Chem. Phys.* **2001**, *95*, 4289.
(48) Forsman, J.; Broukhno, A.; Jönsson, B.; Åkesson, T. *J. Chem. Phys.* **2004**, *120*, 413.
(49) Tildesley, D. J.; Street, W. B. *Mol. Phys.* **1980**, *41*, 85.
(50) Honnell, K. G.; Hall, C. K. *J. Chem. Phys.* **1989**, *90*, 1841.
(51) Honnell, K. G.; Hall, C. K. *J. Chem. Phys.* **1991**, *95*, 4481.
(52) Yethiraj, A.; Curro, J. G.; Schweizer, K. S.; McCoy, J. D. *J. Chem. Phys.* **1993**, *98*, 1635.
(53) Wichert, J. M.; Gulati, H. S.; Hall, C. K. *J. Chem. Phys.* **1996**, *105*, 7669.
(54) Forsman, J.; Woodward, C. E. *J. Chem. Phys.* **2004**, *120*, 506.
(55) Woodward, C. E.; Jönsson, B. *Chem. Phys.* **1991**, *155*, 207.
(56) Yu, Y.-X.; Wu, J. *J. Chem. Phys.* **2002**, *117*, 2368.
(57) Miklavic, S. J.; Woodward, C. E.; Jönsson, B.; Åkesson, T. *Macromolecules* **1990**, *23*, 4149.

MA035508B